PSF Estimation and Image Restoration for Noiseless Motion Blurred Images

WIKKY FAWWAZ A M, TAKUYA SHIMAHASHI, MITSURU MATSUBARA, and SUEO SUGIMOTO
Department of Electrical and Electronic Engineering
Ritsumeikan University
1-1-1, Noji-Higashi, Kusatsu, Shiga
JAPAN

Abstract: In this paper we consider the restoration problem of noiseless linear motion blurred image. The success of restoring this kind of blurred image highly depends on precise estimation of parameters of point spread function (PSF), i.e., motion length and motion direction. In this paper a novel idea for PSF parameters estimation and new approach for motion blurred image restoration are discussed. In motion length estimation, we apply 2-D cepstral analysis used to find periodicity of sinc function whose structure remains in the spectrum of blurred image. In motion direction estimation, we use our proposed, modified discrete Radon transform and 2-D cepstral analysis. The value of estimated length is used as a criteria of which one of the two methods can give better result for a certain length. The estimated PSF parameters are then used in the image restoration. To restore the blurred image, we work in spatial domain by inverting the lower triangular matrix that expresses the degradation process. Finally, test results of our method showed good reproduction of the original image.

Key–Words: modified discrete Radon transform, cepstral analysis, uniform motion blur, and blind image restoration

1 Introduction

Image restoration is one of fundamental problems in image processing. Image restoration aims to reconstruct true image from the degraded image. The most common degradation is motion blur which is caused by relative motion between the camera and the object. Motion blurred image $g(x,\, y)$ can be modeled as an output of 2-D convolutional process between true image $f(x,\, y)$ and PSF $h(x,\, y)$. In noiseless motion blurred image case, the model is given by

$$g(x,\, y) = f(x,\, y) \circledast h(x,\, y) \quad (1)$$

$$= \int_{-\infty}^{\infty}\int_{-\infty}^{\infty} h(x-\zeta, y-\eta)\, f(\zeta, \eta)\, \mathrm{d}\zeta \mathrm{d}\eta \quad (2)$$

In motion blur case, the point spread function has two important parameters, i.e., motion direction and motion length. Parameter estimation of point spread function is very important for restoring the degraded image. Many researchers have involved in this area, but most of them assume that the motion direction is horizontal. In [1] and [2], bispectrum is used in blur identification. PSF parameters identification using power cepstrum is presented in [3], [4], and [5].

The recent works are presented in [6] and [7]. In [7], PSF parameters estimation using 1-D cepstral analysis and Hough transform is demonstrated. Hough transform needs to specify candidate points for the lines. Moreover, since the estimated motion direction is used to rotate the spectrum image, the accuracy of motion length estimation will be affected.

In this paper we proposed a new modified discrete Radon transform and 2-D cepstral analysis for estimating PSF parameters. Compared to the conventional discrete Radon transform, our modified discrete Radon transform can increase the capability of the Radon transform in estimating motion direction. In order to give better estimation, the modified discrete Radon transform and the 2-D cepstral analysis are combined in motion direction estimation. Selection of which method can give better result is determined by the estimated length value. In this paper, motion length is estimated using the 2-D cepstral analysis. We estimate the motion length directly from the 2-D cepstral data.

The blurred image is restored via inverse filtering in spatial domain using the estimated PSF parameters. Firstly, we reformulate the 2-D degradation process into its 1-D form. By using this model, degradation process can be described by a lower triangular matrix. The true image is obtained by inverting the lower triangular matrix, and then multiplying it with the blurred image. In this approach, we apply the inverse matrix to the interpolated pixels along the mo-

tion direction. Bilinear interpolation is used to reinterpolate the estimated true image pixels in motion blur direction. Therefore, the estimated true image can be displayed in the normal view.

2 Motion Blur

In spatial domain, the PSF in (1) can be modeled as [7]

$$h(x,\, y) = \begin{cases} 1/L & \text{if } 0 \le |x| \le L\cos\ \theta;\ y = L\sin\ \theta \\ 0 & \text{otherwise} \end{cases} \tag{3}$$

The frequency response of h is a SINC function, and is given by

$$H(\omega_x,\, \omega_y) = \operatorname{sinc}\left(\pi L(\omega_x \cos\ \theta\ +\ \omega_y \sin\ \theta)\right) \tag{4}$$

As shown in (4), PSF parameters, i.e., motion length (L) and motion direction (θ), are maintained in frequency domain representation of PSF. As we do not know about the PSF, we should estimate the PSF parameters from the blurred image which is expressed as

$$G(\omega_x,\, \omega_y) = F(\omega_x,\, \omega_y)\, H(\omega_x,\, \omega_y) \tag{5}$$

where $G(\omega_x,\, \omega_y)$, $F(\omega_x,\, \omega_y)$, and $H(\omega_x,\, \omega_y)$ are the frequency responses of blurred image, true image and PSF, respectively.

From (4), it is evident that motion blur introduces a sinc structure. This sinc structure also appears in the blurred image, shown by parallel dark lines. The width and the direction of the lines give enough information about motion length and motion direction, respectively, because the width of the lines has a relation with periodicity of sinc structure and direction of the lines is perpendicular to the direction of a motion blur. Therefore, information about PSF parameters can be extracted directly from the blurred image.

3 PSF Parameter Estimation

3.1 Motion Length Estimation

In this paper motion length estimation is done by applying cepstral analysis. Let $g(x,\, y)$, $h(x,\, y)$, and $f(x,\, y)$ denote the blurred image, point spread function, and the original image, respectively. If the blurred image is noiseless, then power density spectra of the blurred image is defined as follows.

$$|G(w_x,\, w_y)|^2 = |F(w_x,\, w_y)|^2 + |H(w_x,\, w_y)|^2 \tag{6}$$

For linear motion blur case, cepstrum can be used to estimate the zero patterns in the frequency response from which one can estimate motion direction and motion length. In this paper two-dimensional cepstrum of $g(x,\, y)$ is used. The power cesptrum is the inverse Fourier transform of the logarithm of the magnitude of $G_k(w_x,\, w_y)$. Thus

$$\hat{g}(x,\, y) = \mathcal{F}^{-1}\ \log\left\{|G(w_x,\, w_y)|\right\} \tag{7}$$

where $\mathcal{F}^{-1}$ is the inverse Fourier transform operator. One of the important properties of the cepstrum is that if two signals are convolved, their cesptrum add. Thus if the noise is neglected:

$$\hat{g}(x,\, y) = \hat{f}(x,\, y) + \hat{h}(x,\, y) \tag{8}$$

To estimate the motion length, frequency zero crossings are observed from (4). Frequency zero crossing happens at $n = m/L$, where $n = \zeta_1 \cos\ \theta + \zeta_2 \sin\ \theta$ and $m = 0,\, \pm1,\, \pm2,\, \pm3, \ldots$. As a result, $\hat{h}$ has a large negative peak at a distance L from the origin [4]. Therefore, motion length is estimated by calculating the distance of the large negative peaks from the origin.

3.2 Motion Direction Estimation

Motion direction is estimated using the Radon transform. The Radon transform is given by [8]

$$g(\rho,\theta) = \int_{-\infty}^{\infty}\int_{-\infty}^{\infty} f(x,y)\, \delta(x\, \cos\theta + y\, \sin\theta - \rho)\, \mathrm{d}x\, \mathrm{d}y \tag{9}$$

In order to apply the Radon transform on a 2-D digital image $g(m,\, n)$ of size $M \times N$, we use the discrete Radon transform. Therefore, we first sample continous variables [9]:

$$x = x_m = x_{min} + m\, \Delta x, \quad m = 0, 1, \cdots, M-1 \tag{10}$$

$$y = y_n = y_{min} + n\, \Delta y, \quad n = 0, 1, \cdots, N-1 \tag{11}$$

$$\theta = \theta_t = \theta_{min} + t\, \Delta\theta, \quad t = 0, 1, \cdots, T-1 \tag{12}$$

$$\rho = \rho_r = \rho_{min} + r\, \Delta\rho, \quad r = 0, 1, \cdots, R-1 \tag{13}$$

where

$$x_{min} = -x_{max} = -(M-1)/2, \tag{14}$$

$$y_{min} = -y_{max} = -(N-1)/2, \tag{15}$$

$$\rho_{min} = -\rho_{max} = -\frac{(R-1)}{2}\, \Delta\rho \tag{16}$$

For our work, we set both Δx and Δy to 1. $\Delta\rho$, T, θ_{min}, and $\Delta\theta$ are set to 1, π, 0, and π/T, respectively. R and ρ_{max} are determined by assuming $\Delta\, \rho = \frac{\Delta x}{\sqrt{2}}$ [9]:

$$R = 2\, \frac{\rho_{max}}{\Delta\rho} + 1 = 2\, \frac{\sqrt{x_{min}^2 + y_{min}^2}}{\Delta\rho} + 1 \tag{17}$$

$$\rho_{min} = -\rho_{max} = -\frac{R-1}{2}\Delta\rho \tag{18}$$

If $\rho = x\cos\theta + y\sin\theta$ and $s = -x\sin\theta + y\cos\theta$, then (9) can be expressed as

$$g(\rho,\,\theta) = \int_{-\infty}^{\infty} g(\rho\,\cos\theta - s\,\sin\theta,\,\rho\,\sin\theta + s\,\cos\theta)\,\mathrm{d}s \tag{19}$$

The discrete Radon transform is achieved by approximating (19) as

$$g(\rho_r,\,\theta_t) \approx \Delta s\sum_{j=0}^{S-1} g(\rho_r\cos\theta_t - s_j\sin\theta_t,\,\rho_r\sin\theta_t + s_j\cos\theta_t) \tag{20}$$

where s_j is a linear sampling of the variable s, and is expressed as

$$s = s_j = s_{min} + j\,\Delta s, \qquad j = 0, 1, \cdots, S-1 \tag{21}$$

$$s_{min} = -s_{max} = \frac{(S-1)}{2}\Delta s \tag{22}$$

$$\Delta s = \begin{cases} \dfrac{1}{|\cos\theta_t|}, & \sin\theta_t \le \sin\dfrac{\pi}{4} = \dfrac{1}{\sqrt{2}} \\ \dfrac{1}{\sin\theta_t}, & \sin\theta_t > \sin\dfrac{\pi}{4} = \dfrac{1}{\sqrt{2}} \end{cases} \tag{23}$$

We assume that each pixel in $g(m,\,n)$ is assgined to its nearest neighbour line. Therefore, the method used in this paper is (fast) nearest neighbour approximation as follows [9].

$\sin\theta > \dfrac{1}{\sqrt{2}}$:

$$g(\rho,\,\theta) = \frac{1}{\sin\theta}\sum_{m=0}^{S} g(m,\,[\alpha\,m + \beta]) \tag{24}$$

where

$$\alpha = -\cot\theta \quad \text{and} \quad \beta = \frac{\rho - x_{min}(\cos\theta + \sin\theta)}{\Delta x\sin\theta}$$

$\sin\theta \le \dfrac{1}{\sqrt{2}}$:

$$g(\rho,\,\theta) = \frac{1}{|\cos\theta|}\sum_{n=0}^{S} g([\alpha\,n + \beta],\,n) \tag{25}$$

where

$$\alpha = -\tan\theta \quad \text{and} \quad \beta = \frac{\rho - x_{min}(\cos\theta + \sin\theta)}{\Delta x\cos\theta}$$

In this paper we consider to modify the discrete Radon transform. First, we define a set $\Theta^{r,t}$ as follows.

$\sin\theta > \dfrac{1}{\sqrt{2}}$:

$$\Theta^{r,t} = \{g(m,\,[\alpha\,m + \beta]) : \theta = \theta_t \text{ and } \rho = \rho_r\} \tag{26}$$

where $m = 0, 1, 2, ..., S-1$

$\sin\theta \le \dfrac{1}{\sqrt{2}}$:

$$\Theta^{r,t} = \{g([\alpha\,n + \beta],\,n) :\, \theta = \theta_t \text{ and } \rho = \rho_r\} \tag{27}$$

where $n = 0, 1, 2, ..., S-1$

In our modified discrete Radon transform, we do not use summation as shown in (24) and (25). For our work, we expect that by using median instead of summation, motion direction can be better estimated. Therefore, we use the following definition:

$$\Upsilon = \text{median}\,(\Theta^{r,t}) \tag{28}$$

By using (26), (27), and (28), (24) and (25) can be expressed as

$\sin\theta > \dfrac{1}{\sqrt{2}}$:

$$g(\rho,\,\theta) = \frac{1}{\sin\theta}\Upsilon \tag{29}$$

$\sin\theta \le \dfrac{1}{\sqrt{2}}$:

$$g(\rho,\,\theta) = \frac{1}{|\cos\theta|}\Upsilon \tag{30}$$

In order to apply the discrete Radon transform, Fourier spectrum of blurred image is treated as an image. To find direction of the lines which appear in the spectrum, the Radon transform is calculated for all directions with $\theta_t = [0,\,\pi - \frac{\pi}{180}]$. We compute the variance of the results for each direction, and then form the variance array V_R as

$$V_R(\theta_t) = \underset{\rho_r}{\text{Var}}\,[g(\rho_r,\,\theta_t)], \quad \theta_t\,\epsilon\,[0,\,\pi - \frac{\pi}{180}] \tag{31}$$

The motion direction is obtained by finding the maximum value of variance array.

Motion direction estimation using cepstral analysis is done by calculating the slope of a line connecting the origin to the first negative value of cepstrum of blurred image. We use both the Radon transform and the cepstral analysis in motion direction estimation.

4 Image Restoration

We assume that degradation process is linear spatially-invariant. Therefore, $M \times N$ blurred image is defined as

$$g(m,n) = \sum_{p=-P}^{P} \sum_{q=-Q}^{Q} h_{p,q}\, f(m-p, n-q) \quad (32)$$

We reformulate (32) to get 1-D degradation process. From (32), the blurred image at m^{th} row is defined as

$$g_m(n) = \sum_{q=-Q}^{Q} h_q\, f_m(n-q) \quad (33)$$

In linear motion blurred case, (33) can be written as (35). Here, for simplification, we first consider that the motion direction is horizontal. As for the motion direction with certain angle, we will describe later in this section.

$$g_m(n) = \sum_{l=-L/2}^{L/2} h_l\, f_m(n-l) \quad (34)$$

$$g_m(n) = \sum_{l=0}^{L-1} \frac{1}{L}\, f_m(n-l) \quad (35)$$

In matrix form, (35) can be written as

$$G_m = H\, F_m \quad (36)$$

where $G_m \in \Re^{N\times 1}, H \in \Re^{N\times N}$, and $F_m \in \Re^{N\times 1}$ are defined by the following matrices

$$G_m = \begin{bmatrix} g(m,1) \\ g(m,2) \\ \vdots \\ \vdots \\ g(m,N) \end{bmatrix} \quad F_m = \begin{bmatrix} f(m,1) \\ f(m,2) \\ \vdots \\ \vdots \\ f(m,N) \end{bmatrix} \quad (37)$$

$$H = \begin{bmatrix} h_0 & & & & & \\ h_1 & \ddots & & & 0 & \\ \vdots & \ddots & \ddots & & & \\ h_{L-1} & \cdots & \cdots & h_0 & & \\ & \ddots & \ddots & \ddots & \ddots & \\ 0 & & h_{L-1} & \cdots & \cdots & h_0 \end{bmatrix} \quad (38)$$

From (36), the restored image is obtained by applying (39) to each row ($m = 1, 2, \ldots M$).

$$\hat{F}_m = H^{-1} G_m \quad (39)$$

H^{-1} in (39) is computed by applying elementary row operations. The restored image $\hat{F}$ is then defined as

$$\hat{F} = \begin{bmatrix} \hat{F}_1^{\mathrm{T}} \\ \hat{F}_2^{\mathrm{T}} \\ \vdots \\ \vdots \\ \hat{F}_M^{\mathrm{T}} \end{bmatrix} \quad (40)$$

where $\hat{F}$ is a $M \times N$ matrix.

As for the motion blurred image with $0 < \theta < \frac{\pi}{2}$, we redefine (32) as

$$z(i,j) = \sum_{p=-P}^{P} \sum_{q=-Q}^{Q} h_{p,q}\, u(i-p, j-q) \quad (41)$$

where $u(i,\, j)$ is the interpolated pixel obtained from original image $F(m,n)$ pixels along the line rotated at motion direction. Therefore, the size of U will no longer equals to that of F. If the size of F is $M \times N$, then U is a matrix with size $I \times J$. I is computed by

$$I = M + \lceil (\tan\theta \times (N-1)) \rceil \quad (42)$$

where $\lceil \cdot \rceil$ indicates ceiling operation.

J should be carefully calculated. Here, we consider various size of the image, i.e., $M \times N$ image.

For $N \leq M$:

$$J = \left\lfloor \frac{1}{\sin\theta} \{(N-1) \times \tan\theta\} \right\rfloor + 1 \quad (43)$$

For $N > M$:

$$J = \left\lfloor \frac{1}{\cos\theta} \{(N-1) - Y\} \right\rfloor + 1 \quad (44)$$

where

$$Y = \frac{1}{\tan\theta} \{((N-1) \times \tan\theta) - (I-1)\} \quad (45)$$

By using (42) - (45), we can treat degradation process which happens at $0 < \theta < \frac{\pi}{2}$ as degradation process in horizontal direction. From (41), the blurred image at i^{th} row is defined as

$$z_i(j) = \sum_{l=0}^{L-1} \frac{1}{L}\, u_i(j-l) \quad (46)$$

In matrix form, (46) can be written as

$$Z_i = H\, U_i \quad (47)$$

where $H \in \Re^{J\times J}$ is defined in the same way as shown in (38). $Z_i \in \Re^{J\times 1}$ and $U_i \in \Re^{J\times 1}$ are defined by the following matrices

$$Z_i = \begin{bmatrix} z(i,1) \\ z(i,2) \\ \vdots \\ \vdots \\ z(i,J) \end{bmatrix} \quad U_i = \begin{bmatrix} u(i,1) \\ u(i,2) \\ \vdots \\ \vdots \\ u(i,J) \end{bmatrix} \tag{48}$$

If (49) is applied to each row of Z, i.e. $i = 1, 2, \ldots I$, then we can obtain the restored image (before reinterpolation) as shown in (50)

$$\hat{U}_i = H^{-1} Z_i \tag{49}$$

$$\hat{U} = \begin{bmatrix} \hat{U}_1^{\mathrm{T}} \\ \hat{U}_2^{\mathrm{T}} \\ \vdots \\ \vdots \\ \hat{U}_I^{\mathrm{T}} \end{bmatrix} \tag{50}$$

However, each element of $\hat{U}$ is the interpolated pixel along the line rotated at motion direction. The true restored image is $\hat{F}$. Therefore, we reinterpolate $\hat{U}$ using bilinear interpolation to get $\hat{F}$. We get that size of $\hat{F}$ after this process is $(M-1)\times(N-1)$.

As for the motion blurred image with $\frac{\pi}{2} < \theta < \pi$, we first reformulate (41) as

$$z_{flip}(i,j) = \sum_{p=-P}^{P} \sum_{q=-Q}^{Q} h_{p,q}\, u_{flip}(i-p, j-q) \tag{51}$$

In the matrix form, (51) can be expressed as

$$Z_{flip} = H\, U_{flip} \tag{52}$$

where U_{flip} is obtained by performing left-right flipping operation to F and then interpolating F along the line rotated at an angle equals to motion direction. As a result, now the Z_{flip} matrix, whose elements are $z_{flip}(i,j)$, is in the form of left-right flipped matrix. In the simulation, we also consider that Z_{flip} matrix is obtained from left-right flipping operation on Z matrix. The matrix size of Z_{flip} is $I \times J$. I and J are defined as

$$I = M + \lceil (\tan\psi \times (N-1)) \rceil \tag{53}$$

For $N \le M$:

$$J = \left\lfloor \frac{1}{\sin\psi} \{(N-1)\times\tan\psi\} \right\rfloor + 1 \tag{54}$$

For $N > M$:

$$J = \left\lfloor \frac{1}{\cos\psi} \{(N-1) - Y\} \right\rfloor + 1 \tag{55}$$

where

$$Y = \frac{1}{\tan\psi} \{((N-1)\times\tan\psi) - (I-1)\} \tag{56}$$

In (53) - (56), $\psi = \pi - \theta$.

By using the same way shown in (46) - (50), we get $\hat{F}$. However, the obtained $\hat{F}$ is a left-right flipped matrix form. The true restored image is obtained by applying left-right flipping operation on $\hat{F}$.

5 Experimental Results

Our experiments are done by using Matlab 6.5.1. In our works, we use the cepstral analysis for estimating motion length (L). We use cepstral analysis and the Radon transform for estimating motion direction. For $L < 15\,\mathrm{pixels}$, cepstral analysis gives better motion direction estimation than the Radon transform does. The maximum error when we use the cepstral analysis is 3 degrees, but it becomes bigger if we use the Radon transform. For $L \ge 15\,\mathrm{pixels}$, cepstral analysis can estimate all values of motion direction (θ) used in the simulation. However, for $\theta \ge 27^o$, the Radon transform gives better result of the estimation. In our simulation, for $L \ge 15\,\mathrm{pixels}$ and $\theta \le 27^o$ the Radon transform fails to estimate (estimation error is more than 10 degrees). In the simulation, our modified discrete Radon transform gives 1-2 pixels more accurate than the discrete Radon transform does.

Tabel 1 shows the computational time of PSF parameters estimation for lenna image (256 x 256 pixels). The experiments are done by using computer with spesification: Intel Pentium M 1.86 GHz and 1 GB RAM. In Tabel 1, DRT denotes the discrete Radon transform that is given by (24) and (25) whereas MDRT denotes our modified discrete Radon transform which is given by (26) and (27).

In our experiment, we combine the cepstral analysis and the modified discrete Radon transform in PSF parameters estimation. The estimated motion length, obtained using the cepstral analysis, is used to determine the better method for estimating motion direction. If $L < 15\,\mathrm{pixels}$, cepstral analysis is used to estimate motion direction. If $L \ge 15\,\mathrm{pixels}$, firstly the cepstral analysis is used. Then, if $\hat{\theta} \ge 27^o$, motion direction is reestimated using the modified discrete Radon transform. Tabel 2 shows the estimation

Table 1: Computational time (in second) needed for PSF parameters estimation

L	θ	Angle Estimation			Length Est.
		Cepst.	DRT	MDRT	Cepst.
15	10	0.0620	9.0620	14.8910	0.1880
24	27	0.0630	9.0470	14.9070	0.0780
44	66	0.0620	8.8600	14.5940	0.0780
53	67	0.0470	9.4530	15.9220	0.0780
79	10	0.1560	11.4680	16.2500	0.6720

Table 2: Estimation of PSF parameters

L	θ	estimated L ($\hat{L}$)	estimated angle ($\hat{\theta}$)
10	4	11	2
15	10	15	8
15	155	15	157
24	27	24	25
25	53	25	51
30	33	30	33
30	116	30	116
41	7	41	6
41	153	41	153
44	66	43	66
53	27	53	27
53	67	53	68
53	71	52	71
63	5	64	5
63	19	63	18
79	10	80	10

result using our method. In simulation, we use 640 x 480 RGB image. Artificially blurred image is obtained by blurring simulation with angles varying from 0 to $\pi - \frac{\pi}{180}$ and length varying from 1-79 pixels. The original image, motion blurred image, and restored image are shown in Fig. 1 - Fig. 5. In this paper we show the results of image restoration in the case of wrong PSF parameters estimation as well as correct PSF parameters estimation. The first case happens when we use $L = 25\,\text{pixels}$ and $\theta = 53^o$ to make the blurred image. The blurred image is restored using the estimated PSF parameters ($\hat{L} = 25\,\text{pixels}$ and $\hat{\theta} = 51^o$). Fig. 3 shows the restored image for the first case. The second case happen when we do simulation using $L = 30\,\text{pixels}$ and $\theta = 33^o$ to make the blurred image. The blurred image is restored using the estimated PSF parameters ($\hat{L} = 30\,\text{pixels}$ and $\hat{\theta} = 33^o$). Fig. 5 shows the restored image for the second case. In the second case, the restored image seems to be closed to the original image.

Figure 1: Original Image

Figure 2: Motion Blurred Image with $L = 25\,\text{pixels}$ and $\theta = 53^o$

6 Conclusion

PSF parameters estimation using the discrete Radon transform and the 2-D cepstral analysis has been demonstrated. Simulation results show the capability of the methods for restoring blurred image. Our method can be applied to any image size, any motion direction, and any motion length. By applying two methods which have their own capability, the accuracy of motion direction estimation using our method is better than by just applying one of the methods. Fortunately, the estimated motion length, used as the criteria, can be obtained in small computational time (see Table 1). Our method can be possibly used for optical character recognition or blurred vehicle plate image recognition because image details can be seen although the estimated PSF parameters are not correct. In future works, we will consider a method to make the restored image becomes clearer, and extend the problem to noisy blurred image case. Although

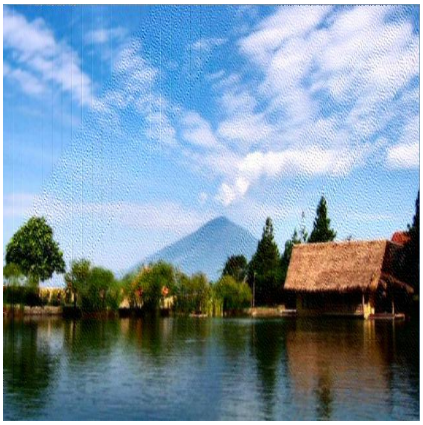

Figure 3: Restored Image using $\hat{L} = 25\,\text{pixels}$ and $\hat{\theta} = 51^o$

Figure 4: Motion Blurred Image with $L = 30\,\text{pixels}$ and $\theta = 33^o$

our modified discrete Radon transform improves motion direction estimation, it takes longer time than the discrete Radon transform. We will consider a technique to overcome this problem.

References:

[1] M. M. Chang, A. M. Tekalp, and A. T. Erdem, Blur identification using the bispectrum, *IEEE Trans. Signal Process.*, Vol.39, No.10, 1991, pp. 2323–2325.

[2] C. Mayntz, T. Aach, and D. Kunz, Blur identification using a spectral inertia tensor and spectral zeros *Proc. IEEE International Conference on Image processing(ICIP)*, 1999.

[3] M. Cannon, Blind deconvolution of spatially invariant image blurs with phase, *IEEE Trans. Acoust. Speech Signal Process.*, Vol.24, No.1, 1976, pp. 56–63.

[4] J. Biemond, R. L. Lagendijk, and R. M. Mersereau, Iterative methods for image deblurring, *Proc. of the IEEE*, 1990, pp. 856–883.

[5] Ioannis M. Rekleities, Optical flow recognition from the power spectrum of a single blurred image, *IEEE International Conference on Image processing(ICIP)*, 1996.

[6] M. E. Moghaddam and M. Jamzad, Motion blur identification in noisy images using fuzzy sets, *Proc. IEEE International Symposium on Signal Processing and Information Technology*, Athens, Greece, 2005.

[7] R. Lokhande, K. V. Arya, and P. Gupta, Identification of parameters and restoration of motion blurred images, *Proc. of ACM Symposium on Applied Computing*, 2006, pp. 301–315.

[8] A. K. Jain, *Fundamentals of Digital Image Processing*, Prentice Hall, 1989.

[9] P. Toft, *The Radon Transform: Theory and Implementation*, Ph.D thesis, Technical University of Denmark, 1996.

Figure 5: Restored Image using $\hat{L} = 30\,\text{pixels}$ and $\hat{\theta} = 33^o$